Ionization of fast foil-excited ion beams in electromagnetic fields

E. P. Kanter, D. Schneider, Z. Vager,* D. S. Gemmell, B. J. Zabransky, Gu Yuan-zhuang,†
Argonne National Laboratory, Argonne, Illinois 60439

P. Arcuni
Argonne National Laboratory, Argonne, Illinois 60439
and Department of Physics, University of Chicago, Chicago, Illinois 60637

P. M. Koch,‡ D. R. Mariani, and W. Van de Water‡
Yale University, New Haven, Connecticut 06511

(Received 3 October 1983)

We report the results of a series of experiments investigating the nature of very-highly-excited states of fast ions emerging from thin foils. The yields of electrons produced by field ionization of these atoms are compared for different projectiles and beam energies. Various field arrangements were used. The consequences for related studies of fast-ion beams penetrating solids are discussed.

I. INTRODUCTION

Fast ions traversing thin solid targets emerge in a variety of excited electronic states. This aspect of ion-solid interactions has made it possible, through beam-foil spectroscopic techniques, to explore the electronic states of a wealth of atoms.[1] Over the course of the last decade, these studies have concentrated mostly on the low-lying excited states of few-electron high-Z atoms. Because of the comparatively small decay rates of higher excited states,[2] and because of the low yields of such states,[3] there has been relatively little spectroscopic work involving principal quantum numbers $n > 10-15$. It has, however, been known for several years that cascades from very high-lying levels play an important role[4] in determining the observed time dependence of measured decay curves.[5] Recently, attention has been focused on this cascade phenomenon.[6] Studies of delayed K-x-ray emission have suggested surprisingly large yields of high Rydberg states[7] and unusual quantum-state populations.[8] Further experiments of this type have shown a strong target thickness dependence of the yields of delayed x rays.[9] These observations have led to speculation[9] about possible formation mechanisms which might be responsible for producing these high Rydberg states. In an effort to better understand these results, we have conducted an intensive series of experiments aimed at measuring the yields and quantum-state populations of high-Rydberg-state atoms formed by beam-foil excitation of fast-ion beams.

An additional motivation for this work came from studies of the foil-induced dissociation of fast molecular ions. Measurements of the energy and angular distributions of hydrogen fragments resulting from the foil-induced dissociation of 3.63-MeV HeH^+ beams[10] had shown remarkably similar distributions when both H^0 and H^- fragments were observed. It was postulated[11] that this was an indication for the formation of dissociative molecular Rydberg states as the fragments exit the foil. To test this hypothesis, we sought to measure directly the yields of high Rydberg states of hydrogenic H and He atoms and ions produced by beam-foil excitation of H^+, He^+, H_2^+, and HeH^+ beams. The approach we used involved static electric field ionization of components of the beam emergent from the target in Rydberg states.

II. ELECTRIC FIELD IONIZATION

Electric field ionization is a very efficient method of detecting high-Rydberg-state atoms, but the details of field ionization differ according to whether the system is "hydrogenic" or "nonhydrogenic." It is well known that in an external applied electric field ionization rates of the parabolic substates of highly excited hydrogen atoms calculated with the use of nonrelativistic theory rise monotonically, and rapidly, with increasing field strength. The increase is so rapid that the concept of a threshold field F_t for ionization is justified. The pure Coulomb-Stark potential $V(r) = -Z/r + Fz$ for the nonrelativistic hydrogen atom (or hydrogenic ion with nuclear charge Z) allows separation of the Schrödinger equation in parabolic coordinates.[2] The "classical" threshold field $F_t(cl)$ for a given parabolic substate $(n_1, n_2, |m|)$, where the principal quantum number $n = n_1 + n_2 + |m| + 1$, corresponds to that value when the atomic electron can escape classically over the potential barrier which exists in one (usually called η) of the parabolic coordinates.[2] Of course, quantal tunneling through the barrier allows field ionization to occur below $F_t(cl)$.[2] Recent field ionization measurements[12,13] with resolved parabolic substates in the $n = 30,40$ manifolds of hydrogen have confirmed the validity of numerical calculations in this tunneling regime. Theoretically, the threshold field F_t has an overall $Z^3 n^{-4}$ scaling, with a constant of proportionality that depends on the parabolic substate. Useful classical values for the $(n_1, n_2, |m|)$ dependence of this constant have been presented graphically.[14] In a given n manifold, the Stark-shifted substate $(0, n-1, 0)$ that lies lowest in energy has the lowest threshold, $n^4 F_t(cl)/Z^3 \sim 0.13$ a.u. The Stark-shifted substate $(n-1, 0, 0)$ that lies highest in energy has the highest threshold $n^4 F_t(cl)/Z^3 \sim 0.35$ a.u. [The atomic unit of the electric field is $F(\text{a.u.}) = 5.142\,250(17) \times 10^9$ V/cm (Refs. 2, 12, and 13).] Stark-shifted substates lying in energy between these extremal states have classical proportionality constants lying between these limits. For quantal tunneling ionization rates between 10^5-10^8 s^{-1},

the ionizing field was observed[12,13] to be about 15% below the classical value.[14]

If, as in the present experiment, individual substates were not resolved in a beam containing an unknown mixture of substates, the concept of an approximate threshold field for ionization of a given n manifold is still useful. This was well established in a number of early fast-beam experiments with highly excited hydrogen atoms.[15] An approximate value for the threshold field in this case is given by $n^4F_t/Z^3 \sim 1/8$ a.u. For the purposes of the present paper, this is the assumed threshold field for ionization of one-electron atoms or ions by a static electric field.

In nonhydrogenic Rydberg-state atoms, the situation is much more complicated. The interaction of the Rydberg electron with its ionic core induces a coupling between different parabolic (hydrogenic) channels, causing Stark potential curves with the same value of the magnetic quantum number $|m|$ to avoid crossing.[16] The lower the value of $|m|$, the larger, in general, is the avoided crossings, and the more nonhydrogenic is the field ionization behavior. The threshold for ionization is lowered to the "saddle-point" limit, which for $m=0$ and unit core ionic charge is given by $n^4F_{sp}=1/16$ a.u.[16] Let us call this saddle-point ionization, or that due to the effects of atomic structure. The actual F dependence of the rate of ionization in the neighborhood and beyond this threshold, of course, depends essentially on the details of the Stark structure of the atom in question. Furthermore, if the ionizing electric field changes with time, as, for example, in the rest frame of fast atoms flying through a region where the electric potential varies spatially, dynamic effects at the avoided crossings also may greatly influence the field ionization process.[16,17]

The first observation of the electric field ionization of hydrogen came in 1930 from studies of the Stark effect in the Balmer spectrum with a canal ray light source.[18] In the early 1960's, there was a great deal of work studying the field ionization of fast beams in connection with the thermonuclear fusion research program.[19] Most of that work involved 10—100-keV protons or deuterons incident on gaseous or vapor targets.[15,19] Strong fields ($\sim 10^5$ V/cm) were used to ionize high-n atoms and the resulting ions were detected. There was some work with higher-energy primary beams[20] but, again, mostly with gaseous (or plasma) targets and using strong fields. The work with solid targets which has been reported to date[21,22] has all been at beam energies less than 100 keV and has used comparatively strong fields, concentrating on states with principal quantum numbers less than 25. All of these experiments detected ions.

There is, however, considerable advantage in detecting the ionized electrons. For high beam velocities the orbital velocities of these electrons can be neglected and, therefore, they will be observed in the laboratory to be moving with the beam velocity (with laboratory energy $\sim 1/2000$ of the projectile energy for incident protons). For example, one would expect to observe $\sim$400-eV electrons from the ionization of 750-keV hydrogen Rydberg atoms. With quite moderate fields, it is easy to separate such electrons from the more intense primary beam and detect them with essentially unity efficiency. This permits studies of much higher principal quantum numbers (limited only by stray fields). It is these highly excited states ($n > 40$) which are so important to the delayed K-x-ray problem. The mechanisms that produce these states are also surely at work in the related phenomenon of convoy electron production.[23]

III. IONIZATION IN A MICROWAVE FIELD

Ionization in a microwave electric field is also a very efficient method of detecting Rydberg atoms, but much less is known about its details than is known for ionization in a static electric field. The present state of understanding can be found in Refs. 13 and 24—26, from which the following comments are drawn. They are meant to emphasize the use of microwave ionization as a detection process rather than to reveal the subtleties of the underlying physical processes leading to ionization in an oscillatory electric field.

When highly excited hydrogen atoms are exposed to tens or hundreds of cycles of a microwave field in a waveguide or resonant cavity, it is observed that ionization begins to take place above a certain microwave power. This corresponds to an ionization threshold value of the amplitude F_0 of the microwave electric field $F(t)=F_0\cos(\omega t)$. (Elementary calculations show that the influence of the magnetic component of the microwave field is negligible.) At some larger value of F_0, an experimental ionization signal saturates when the probability for ionizing all atoms exposed to a certain number of cycles of the microwave field approaches unity. Thus far, experiments studying microwave ionization of highly excited hydrogen atoms have not studied the ionization behavior of individual (parabolic) substates.[13,24—26] They have used fast beams of hydrogen atoms with an unknown, but undoubtedly large, possibly statistical, distribution of substates.

Two important and physically significant parameters that emerge in a classical theory[27] for microwave ionization are F_0/F_{at} and ω/ω_{at}. The first is the ratio of the field amplitude to the Coulomb binding field experienced by the atomic electron in a Bohr orbital with principal quantum number n. The second is the ratio of the microwave frequency ω to the Bohr orbital frequency ω_{at}. For a hydrogenic system with nuclear charge Z, $F_0/F_{at}=n^4F_0/Z^3$ a.u. and $\omega/\omega_{at}=\omega(Z/N)^3$ a.u. The atomic unit of angular frequency is 4.134×10^{16} s^{-1}.[2] The first parameter expresses the same n and Z scaling as that for static electric field ionization. The second parameter, however, relates frequency scales. When $\omega/\omega_{at} \ll 1$, the temporal variation of the microwave field is quasistatic compared to the rapid orbital motion of the electron. One naturally expects this situation to be most like a static field. When $\omega/\omega_{at} \gg 1$, the jiggling of the electron at the microwave frequency is very rapid compared to the Bohr orbital frequency and one expects the two motions to be relatively decoupled. When $\omega/\omega_{at} \sim 1$, however, the two motions will certainly be most strongly coupled.[27]

In the present experiments microwave ionization was done at the single frequency $\omega/2\pi=9.91$ GHz and for values of F_0 which corresponded to ionization of hydro-

gen atoms with n values much below $n=90$. Since it is only at this large value of n that this microwave frequency makes the parameter $\omega/\omega_{at}\sim 1$, the microwave ionization could be characterized as quasistatic for the much lower n values covered in the present data. In the quasistatic limit, what data do exist[13,24–26] suggest that hydrogen atoms have an ionization threshold near $n\,^4F_0\sim 0.1$ a.u. and that ionization signals saturate at or before $n\,^4F_0\sim 0.14$ a.u. We have assumed that the n and Z scaling given above may be used to infer ionization thresholds for high excited He^+ ions from those for highly excited hydrogen atoms.

Recent experiments[24–26,28] have shown that the microwave ionization behavior of nonhydrogenic Rydberg atoms is very different from that in a one-electron system. As in the static field ionization case, the interaction of the Rydberg electron with its core ion leads to much more complicated dynamics. Ionization curves for helium atoms prepared in $He(1sns)^3S_1$ Rydberg states have revealed rich structure, such as bumps and plateaus, which have been at least partially analyzed and explained with a quasistatic model.[24–26] In particular, in the quasistatic domain, the microwave ionization threshold for these states was correlated with the value of the field needed to Stark shift the initial level into the region of its first avoided crossings with Stark levels from the adjacent n manifold. This field scales approximately as n^{-5}.[24–26,28] Indeed, the n^{-5}-scaling law observed[28] for the threshold microwave field amplitudes for sodium atoms prepared in ^2S and ^2D Rydberg states support this quasistatic analysis.

Because of the relatively high range of beam energies used in the present experiments with light atomic and molecular foil-excited ions, it is expected that the ions or ionic fragments leaving the foil were predominantly hydrogenic, i.e., one-electron systems. Therefore, the microwave ionization analysis centered on the behavior described above for hydrogenic systems in the quasistatic domain.

IV. CONVOY ELECTRONS

A prominent feature observed in the energy spectrum of electrons emitted in the forward direction from thin foils[23] and gas targets[29] under fast-ion bombardment is a sharp cusplike peak occurring at an energy where the electron velocity matches the velocity of the emerging ions. For fast light ions incident on gas targets, these "cusp" electrons are believed to originate predominantly from the capture of target electrons into continuum states of the fast-moving projectile.[30] In the case of solid targets, the term "convoy electrons" is applied to this phenomenon. Intense experimental and theoretical efforts have been directed towards understanding these phenomena during the past ten years.[31] For ion-atom collisions, the production of cusp electrons by fast bare projectiles is described in terms of the electron-capture-to-the-continuum (ECC) model. Calculations[32] based on this model give generally good agreement with experiments using gas targets.[33] For convoy electron production in ion-solid collisions, attempts have been made to describe the observations by last-layer capture (ECC) and in terms of a "wake-riding" model.[34] Neither of these models has been successful in describing the systematics (peak width, yields, target dependence, projectile dependence, etc.) of convoy electron observations. Most of the experimentally observed features still lack satisfactory explanation.[31]

In convoy electron measurements it is customary to pass the projectiles emerging from the target through an electrostatic (or magnetic) spectrometer to observe the electrons emitted from the target in the beam direction. This observation, and the difficulties alluded to above, prompted us to speculate about the extent to which field ionization (in the spectrometer) of Rydberg atoms in the beam emerging from the target could be affecting observations on convoy electrons. If electron capture can occur into continuum states lying just above the ionization threshold of the projectile, capture into bound states lying just below the ionization threshold also can be expected to occur with comparable probability (see, for example, Refs. 30, 31, 33, and 35). If convoy electrons and Rydberg atoms were to emerge from the target in comparable numbers, the intensity and shape observed for the cusp peak would depend critically on experimental parameters such as the spectrometer fields (their magnitudes and directions), the quality of the vacuum, flight distance from target to spectrometer, etc. Our apparatus was designed to allow us to distinguish electrons produced by field ionization of Rydberg atoms from convoy electrons originating at the target. A preliminary account of our efforts to distinguish between these two sources has already been given.[36]

V. EXPERIMENTAL APPARATUS

These experiments used ion beams accelerated by Argonne's 4.5 MV Dynamitron. Typical ions were H^+, H_2^+, He^+, HeH^+, and Ne^+, at energies ranging from 500 keV to 4 MeV. Some additional measurements were performed with 125-MeV S^{14+} ions accelerated by the Argonne tandem-linac accelerator system. Some variations on the basic apparatus were made for the different field geometries employed.

A. Static field measurements

After acceleration, the ions were analyzed magnetically and collimated so that upon entering a 28-in. diameter aluminum vacuum chamber (2×10^{-7} Torr), the beam-spot size was 1 mm and the angular divergence was 0.11 mrad (full width at half maximum).[37] In the chamber (see Fig. 1) the beam first traversed a monitoring system consisting of a rotating chopper and detector for scattered projectiles. The chopper and detector system was calibrated against a biased Faraday cup so that the ion beam current could be monitored absolutely. The beam then passed consecutively through two sets of mutually orthogonal (Y and X) electrostatic deflectors, a foil target, a further set of electrostatic deflectors (X), the entrance aperture of a 45° parallel-plate electron spectrometer,[38] and finally a hole drilled in the back plate of the spectrometer. The spectrometer was located so as to view electrons emerging from the target parallel to the incident beam and was oriented so that analyzed electron trajectories lay in

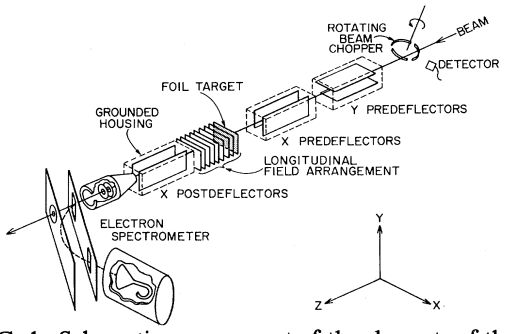

FIG. 1. Schematic arrangement of the elements of the experimental setup inside the target chamber used for static field measurements.

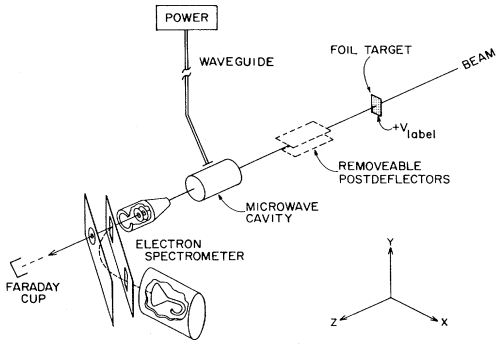

FIG. 2. Schematic arrangement of the elements of the experiments setup inside the target chamber used for microwave field experiments.

the X-Z plane. The analyzed electrons were detected with either a channeltron or an open electron-multiplier tube. The housings for the deflectors and spectrometer were all electrically grounded. Additionally, the target was electrically isolated and held either at a fixed elevated potential ($\sim$50—100 V) or grounded. The 3.7-mm diameter entrance nozzle of the spectrometer abutted the postdeflector housing and was located 15.8-cm downstream from the target. An entrance aperture in the housing of the postdeflector limited its angular acceptance to $\pm$180 mrad.

Except for the additional electrostatic deflector plates, this apparatus is quite similar to that used by other workers studying cusp-electron spectra.[29,31,33] We took special caution to be certain that no electrons would be created in the spectrometer by stray beams striking any of the interior metal surfaces. We used large entrance and exit apertures in the spectrometer, sacrificing energy and angular resolution ($\sim$8% and 24 mrad, respectively) to minimize such background contributions. As a further precaution, in addition to an optical alignment, the X and Y predeflectors were used to "trim" the direction of the incident ion beam, after collimation, to guarantee that the raw beam (without target) was centered through the spectrometer. Using this procedure, the tuned beam was increased in intensity and passed through the spectrometer, without a target. The observed count rate was less than 3 counts/sec, several orders of magnitude lower than the rates during the actual measurements with targets which used lower beam intensities. As an extra test, the spot size of the beam was increased to 2.5 mm by increasing the sizes of the beam-defining apertures. This was intended to simulate the broadening of the beam due to multiple scattering in the target. The observed count rate remained <3 counts/sec.

B. Microwave field measurements

A slightly different experimental arrangement was used for the measurements using microwave fields (see Fig. 2). After passing through a collimation system and beam normalizing chopper similar to that described above, the beam entered an 18-in. diameter aluminum vacuum chamber. Inside this chamber the ion beam passed first through a thin foil target and then through a set of removable electrostatic postdeflectors. Following the postdeflectors was a cylindrical copper microwave cavity, 2.66 cm in radius, with its 4.96-cm long axis aligned with the beam. The cavity was closed by two 0.48-cm thick endplates which had 0.32-cm diameter holes for the beam to enter and exit the cavity. The distance from the target to the entrance endplate of the cavity was 11.04 cm. After exiting from the cavity, the beam traversed 4.34 cm before entering a 45° parallel-plate electron spectrometer, identical to that used in the static field measurements. The cavity, which was operated in the TM_{020} mode[25,26] at 9.91 GHz, had a $Q\simeq$15 000. In this mode, the Rydberg atoms traversing the cavity with the beam, encountered a rapidly oscillating longitudinal electric field (either parallel or antiparallel to the beam). For the beam velocities used in these experiments, this field would oscillate $\sim$50—100 times during the dwell time of a projectile in the cavity. By varying the microwave power in the cavity (from 0 to 18.4 W maximum) we were able to continuously adjust the maximum electric field from 0 to $\sim$2.8 kV/cm.[25,26] The entire apparatus in the 18-in. chamber, consisting of target, removable postdeflectors, microwave cavity, and electron spectrometer, was surrounded by mu-metal to shield the analyzed electrons from stray magnetic fields.

C. Differential field measurements

Additional experiments were carried out with longitudinal electric fields extending from the target exit downstream. The longitudinal electric field was formed by biasing the target and connecting a resistor chain to a set of ten equally spaced parallel electrodes ending at an electrical ground 1.7 cm beyond the target (on the beam exit side). With this field arrangement, a digital lock-in technique was used to perform differential measurements.[39] In these experiments, a small (typically $\pm$0.5—3 V) square wave (1—5 kHz) was added to the target bias voltage. In separate scalers we counted the residual spectrometer ionization signal during the positive and negative phases of the applied square wave. The difference of those scalars, as a function of the applied longitudinal field, is a measure of the derivative of the quench curve.

VI. RESULTS AND DISCUSSION

Figure 3 shows a typical joint distribution, measured with the apparatus shown in Fig. 1. This distribution was obtained with a 3-MeV He^+ beam and a 2-$\mu g/cm^2$ carbon target. The experimental procedure was as follows. First, with all deflector plates grounded, an electron spectrum was recorded and the cusp peak identified. Then, the yield of cusp electron was maximized by applying voltages to the predeflectors, thereby fine tuning the direction of the incident ion beam. (In this way, a limited angular distribution for the cusp electrons was also obtained.) Figure 3(a) shows the electron energy spectrum obtained after this alignment procedure. Next, equal and opposite voltages were applied to the postdeflector plates producing a transverse electric field. Figure 3(b) shows the relative yield of electrons detected as a function of the fields in the postdeflector and the spectrometer. The deflection of the emerging projectiles in these measurements was negligible (for He^{2+} it was $\sim 1/4000$ of the deflection of convoy electrons coming from the target).

Except for the beam-velocity electrons, the electron yield is seen to vary with the postdeflector field as expected for electrons originating from the target. The behavior of the electrons analyzed near the beam velocity is, however, quite different. There appear to be two distinct components contributing to the cusp peak. The first component varies with the postdeflector field in the manner expected for target electrons. The second component behaves quite differently. It is much less affected by the postdeflector field than are the electrons originating at the target and it appears as a "ridge" in Fig. 3(b).

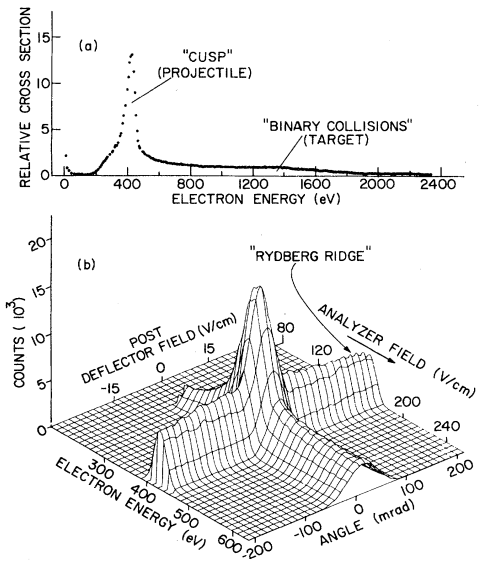

FIG. 3. Electron distributions measured for 3-MeV He^+ incident on a 2-$\mu g/cm^2$ carbon foil. (a) Electron energy distribution obtained in the forward direction. The peaks corresponding to cusp electrons and to binary encounters with target electrons are marked. (b) Distribution of electrons detected as a function of the postdeflector and spectrometer fields. The energy scale applies to electrons from the target. The angle scale applies only to cusp electrons ($\sim$400 eV) coming from the target. The distribution in (a) was derived by dividing the measured electron counting rates by the electron energies in order to take into account the energy dependence of the spectrometer acceptance. This correction has not been applied in (b).

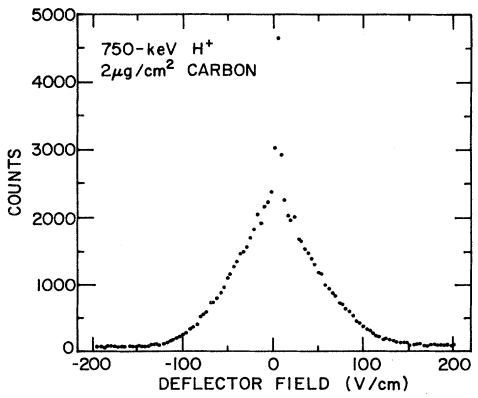

FIG. 4. Electron distribution measured along the Rydberg ridge for 750-keV protons incident on a 2-$\mu g/cm^2$ carbon foil. The field of the spectrometer was held constant at a value corresponding to the energy of the cusp peak at zero deflector field.

We have identified the ridge electrons in Fig. 3 as arising from Rydberg atoms created either inside or at the exit surface of the target foil when emerging helium projectiles capture target electrons into bound states. These atoms fly undeflected (He^0) or almost undeflected (He^+ and He^-) into the electron spectrometer which, if set to analyze $\sim$400-eV (cusp) electrons, contains an electric field of 170 V/cm. For He^0 Rydberg atoms this field reduces the ionization lifetime to less than 1 nsec for $n \simeq 50$ (and shorter lifetimes for higher principal quantum numbers).[16] Since 3-MeV helium atoms travel about 1.2

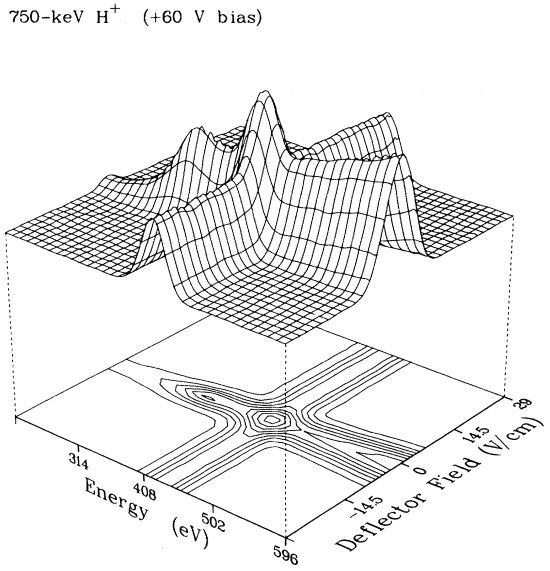

FIG. 5. A joint electron distribution, as in Fig. 3(b), for 750-keV proton bombardment of a 2-$\mu g/cm^2$ carbon target. A + 60 volt bias potential was applied to the target, lowering the energies of electrons produced at the target by 60 eV.

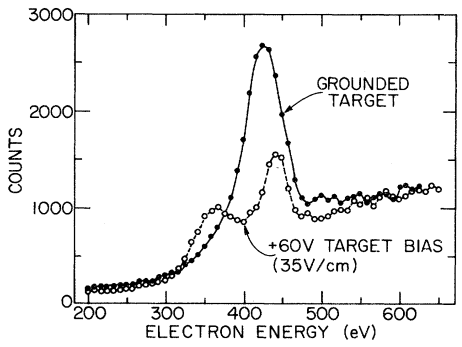

FIG. 6. Distributions of apparent energies for 0° target electrons resulting from 750-keV proton impact on a 2-μg/cm^2 carbon foil. The solid curve was measured with the target grounded. The dashed curve is an energy spectrum from the joint distribution of Fig. 5 for zero postdeflector voltage, with +60 volts bias applied to the target.

cm in a nanosecond, we can expect that the spectrometer field will ionize all Rydberg atoms with n values greater than about 50. For hydrogenic He^+, the corresponding n is slightly higher (~ 80) because of the Z^3 dependence of the classical threshold field.[14] The weaker electric field in the postdeflector [up to about 30 V/cm for the data shown in Fig. 3(b)] will only ionize Rydberg atoms with much higher principal quantum numbers than will the spectrometer field.

Spectra measured with stronger postdeflector fields show, as expected, that the "Rydberg ridge" decreases with increasing field as Rydberg atoms are then field ionized in the postdeflector, and the resulting electrons are swept out of the beam by that field, before reaching the spectrometer entrance. Figure 4 shows a scan, taken along the ridge, of the postdeflector field with the electron spectrometer fixed to analyze cusp electrons. One sees that at a postdeflector field of 170 V/cm, where this field matches the field in the specrometer, the ridge height is about $\frac{1}{20}$ of its value at a field of 30 V/cm.

Closer inspection of distributions such as that in Fig. 3(b) shows that the center of Rydberg ridge is displaced upward in apparent energy by about 18 eV from the energy of the cusp peak. This shift of apparent energy can be seen more clearly in experiments where the target is biased at a fixed potential above ground, thereby lowering the energies of electrons emerging from the target and entering the spectrometer (see Fig. 5). Figure 5 shows a joint distribution measured with the target biased at +60 V. One sees that although the energies of electrons originating from the target are lowered by 60 eV, the Rydberg ridge is unaffected by this bias potential. When this bias is applied to the target, there is a weak (~ 35 V/cm) nonuniform electric field in the region between the target and postdeflector housing which defocusses target electrons and ionizes some Rydberg atoms with $n \gtrsim 75$. An energy spectrum, from this joint distribution, is shown in Fig. 6, measured with the postdeflectors grounded. The apparent energy shift of the Rydberg component is clearly seen here. The upward shift in apparent energy can be explained as being due to the field ionization occurring after the Rydberg atoms penetrate a short distance into the spectrometer. The observed 18-eV shift corresponds to a penetration depth of 2 mm. This distance is reasonable in view of the spatial extent of the transition field at the 3-mm entrance to the spectrometer.

In order to confirm that the beam-velocity electrons which originate in the spectrometer field were not caused by production of ECC electrons in collisions with residual gas atoms, measurements such as those shown in Fig. 6 were repeated with progressively higher gas pressures in the target chamber (see Fig. 7). It was found to be necessary to deteriorate the vacuum by more than two orders of magnitude before observing such electrons from gas collisions. Electron spectra measured with chamber pressures up to 1×10^{-5} Torr showed no dependence on the gas pressure. At a pressure of 7×10^{-5}, however, one notes an increase in the yield of electrons at energies between the cusp and Rydberg peaks. This signifies the production of cusp electrons in the region between the target (at high potential) and the spectrometer (at ground potential) due to collisions of the exiting primary ion beam with gas atoms.

We have observed this phenomenon for a wide range of projectiles, from slow light ions (500-keV H^+) to fast heavy ions (125-MeV S^{14+}).[40] In the latter case, the range of principal quantum numbers to which the experiments were sensitive was $250 < n < 650$. In all cases, a substantial component is observed due to field ionization of highly excited atoms in the spectrometer field.

While the measurements described above demonstrate the presence of field-ionizing Rydberg atoms in the exiting beam, they do not give any quantitative information about the quantum-state populations of these atoms. In order to gain such information, it is necessary to decouple the field which induces ionization from that which energy analyzes the resulting electrons. Ideally, the ionizing field should not defocus the resulting electrons nor contribute to their energy spread.

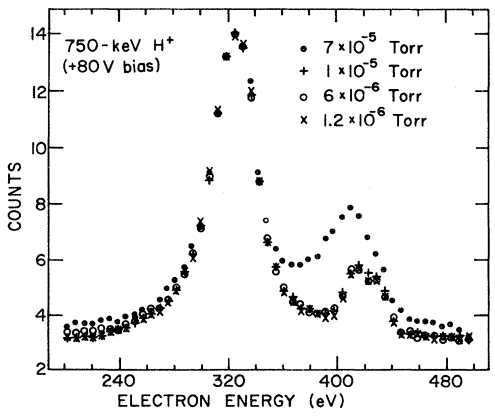

FIG. 7. A comparison of 0° electron energy spectra for 750-keV proton impact on a 2-μg/cm^2 biased carbon target. Spectra are shown for several different values of the pressure in the 18-in. vacuum chamber.

A. Microwave fields

The rapidly oscillating longitudinal electric field of the TM_{020} microwave cavity meets both of these requirements. Bayfield and Koch[41] first demonstrated the use of intense microwave fields to induce multiphoton ionization and excitation of highly excited hydrogen atoms. Those experiments were followed by more detailed measurements, aimed at studying the intensity, frequency, and quantum-state dependencies of these phenomena.[24–26,42,43] These techniques have since been exploited as an efficient means of detecting high-Rydberg-state atoms in fast beams.[12,24–26,44–46]

By inserting a microwave field between the target and spectrometer, we were able to separate the ionizing and analyzing fields. Figure 8 shows a typical joint distribution comparing electron energy spectra as a function of microwave power. In these measurements, the target was held at a positive bias potential to label electrons originating there. At zero microwave power, the electron energy spectrum shows two distinct peaks. The convoy electron peak, lowered in energy by the label voltage, and the peak, shifted up in apparent energy, due to field ionization of high-Rydberg-state atoms in the spectrometer field. When the microwave power is switched on, the electric field in the cavity induces ionization of high-Rydberg-state atoms in the beam. As the power is increased, this field surpasses that in the spectrometer and the field-ionization signal is observed at an electron energy corresponding to the beam velocity. Figure 9 is an electron energy spectrum for 2-MeV He^+ taken with low microwave power (10 mW). At this low power level, the field in the cavity (65 V/cm) is lower than the electric field in the electron spectrometer (115 V/cm). As a result, there is a residual contribution of atoms which do not ionize in the microwave field but are ionized after penetration of the spectrometer field. One clearly observes (in Fig. 9) the three distinct peaks corresponding to convoy electrons (shifted by the applied target bias to 207 eV), microwave-induced ionization (272 eV), and spectrometer-induced ionization (shifted up in apparent energy to 290 eV). As the applied microwave power is increased the spectrometer-induced field ionization signal is quenched, while the microwave-induced ionization signal grows rapidly with the applied power soon surpassing the convoy yield. In contrast, the convoy peak is virtually unaffected by the microwave power, (see Fig. 10) both in amplitude and in width.

The microwave-ionization peak is broadened in energy slightly with increasing microwave power. This can be understood since the electrons contributing to this peak can be produced at different phases. Quantitative estimates of this effect predict a maximum energy shift of ± 20 eV for 400-eV electrons produced in a 10-GHz field with a maximum strength of 1 kV/cm, in agreement with the data.

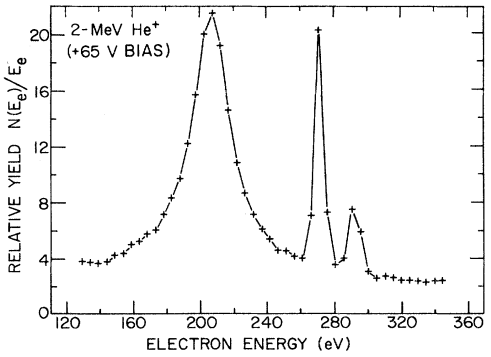

FIG. 9. A spectrum of apparent electron energies for 0° electrons from a foil-excited 2-MeV He^+ ion beam. After exiting the 2-$\mu g/cm^2$ target, biased at $+65$ volts, the ions passed through a low-power (10 mW) microwave cavity where the maximum electric field was ~ 66 V/cm. The field in the spectrometer was 116 V/cm to analyze 290-eV electrons.

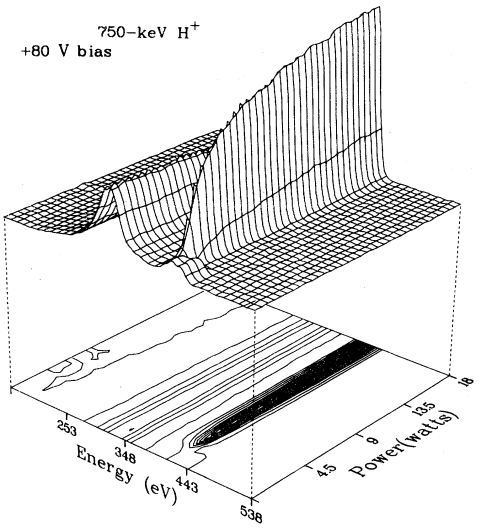

FIG. 8. Joint distribution of electron energy spectra, measured with the spectrometer, as a function of the microwave power supplied to the cavity. The beam was 750-keV H^+ incident on a 2-$\mu g/cm^2$ carbon foil.

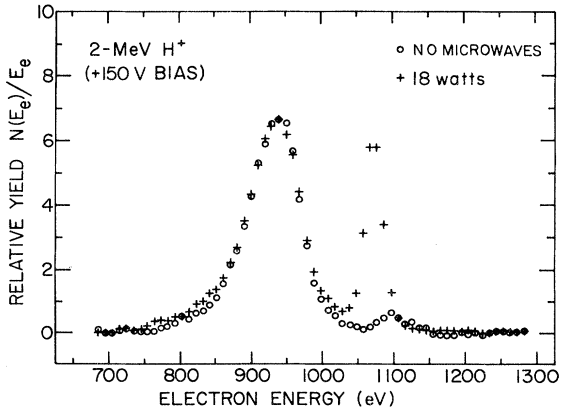

FIG. 10. Comparison of electron energy spectrum following microwave-induced ionization at full power (18 Watts) to an equivalent spectrum with the microwave power off. The ion beam was 2-MeV H^+ on a carbon foil held at $+150$ volts.

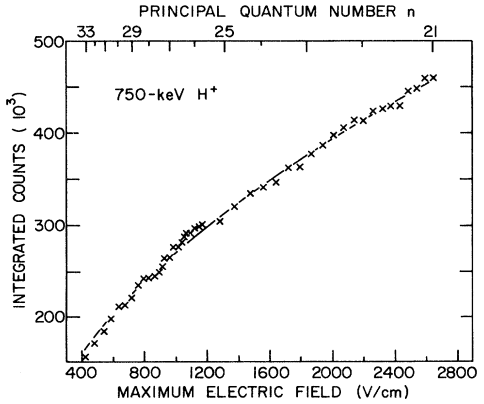

FIG. 11. Integrated yield of the microwave-induced ionization peak observed in the 0° electron energy spectrum for 750-keV H^+ as a function of the maximum electric field in the microwave cavity. The upper abscissa represents the principal quantum numbers corresponding to the saddle-point threshold. The dashed line is the result of the fitting procedure described in the text.

Joint distributions, such as that in Fig. 8 were measured for beams of H^+, H_2^+, and He^+ at energies between 0.5—2.0 MeV. These distributions were analyzed by slicing the joint distributions into individual energy spectra at fixed microwave power. After subtraction of a smooth background of secondary electrons, the peak integrals of the convoy and microwave ionization contributions to the spectra were extracted. Figure 11 shows the results of such an analysis for 750-keV H^+ including data from both coarse (0—18 W) and fine (0—1 W) scans of the microwave power.

The average behavior of these curves can be fitted by assuming simple power laws in n, the principal quantum number, for both the threshold scaling law and the final state population probability for those Rydberg atoms entering the microwave cavity. If we postulate a population distribution given by

$$P(n)=a/n^r \tag{1}$$

and a threshold scaling law

$$F=bZ^3/n^m , \tag{2}$$

then it is easy to show that the integral ionization yield at the field strength F will be given by

$$I(F)=[a/(r-1)](F/b)^{(r-1)/m} . \tag{3}$$

For $m=4$ and $r=3$, this reduces to a square-root dependence on the field. We have adopted (see Sec. III) the values $b=6.14\times10^8$ V/cm (Refs. 24—26) and $m=4$ and from fits to the measured yield curves, we extract the parameter r. Table I shows a summary of these results. The errors quoted in the table include both fitting errors as well as a 20% uncertainty in the value of b. (See Section III.) Combining all of the data, we find $r=3.08\pm0.12$.

On the basis of these results, we chose $r=3$ and refit each of the curves to a $\sqrt{F}$ dependence. The result of those fits is the parameter a in Eq. (1). This parameter, normalized to the incident flux of projectile nuclei, is presented in Table I for each of the fitted distributions. The uncertainties quoted in the table for this parameter result mainly from the large uncertainty assumed for the critical threshold constant b. Also shown in Table I are published values of the one-electron fractions of the emergent ion beams. For the H^+ data, we have made comparisons with measurements of the neutral yield of hydrogen.[47] The values for He are the He^+ fractions given in the tables of Armstrong *et al.*[48] For H_2^+, we include the observed enhancement of the H^0 yield in the published value.[49]

We have also investigated the yields of convoy electrons observed in these experiments. We have extracted, from the joint distributions Y_c, the yield per incident nucleus of convoy electrons observed within the angular acceptance of the electron spectrometer (acceptance half-angle $=0.47°$). The yields we extract from these data are in excellent agreement with the reported "restricted yields" given by Laubert *et al.*,[50] when the latter values are scaled to account for the different angular acceptance employed in those measurements (these scaled values are shown in Table I). The yield of convoy electrons serves as a convenient comparison to test the yields of Rydberg atoms which we extract. It is reasonable to assume that the formation mechanisms which lead to convoy electron production are the same mechanisms at work in the production of the very highly excited *bound states* which we observe through field ionization. As a result, the velocity- and projectile-charge dependence of both the convoy and Rydberg yields should be the same. Because we measure the yield of convoy electrons in a restricted angular acceptance, this yield should increase as the square of the beam velocity, reflecting the narrowing of the convoy electron angular distribution. Figure 12 shows a comparison of the ratio Y_c/a as a function of the square of the beam velocity. The proton data show good agreement with a

TABLE I. Summary of analysis of microwave data.

Ion	Energy (MeV)	r	a	Single-electron yield	Y_c	Ref. 50
H^+	0.5	2.94±0.25	$2.3\pm0.6\times10^{-4}$	2.5×10^{-3}	2.0×10^{-7}	6.3×10^{-7}
H^+	0.75	3.33±0.29	$2.9\pm0.5\times10^{-4}$	1.1×10^{-3}	4.0×10^{-7}	3.7×10^{-7}
H^+	2.0	3.31±0.29	$1.7\pm0.5\times10^{-5}$	1.0×10^{-4}	7.4×10^{-8}	1.0×10^{-7}
He^+	2.0	3.00±0.25	$1.3\pm0.4\times10^{-2}$	6.3×10^{-2}	2.4×10^{-6}	4.2×10^{-6}
H_2^+	1.5	2.94±0.25	$5.6\pm1.7\times10^{-4}$	2.8×10^{-3}	3.3×10^{-7}	
		3.08±0.12				

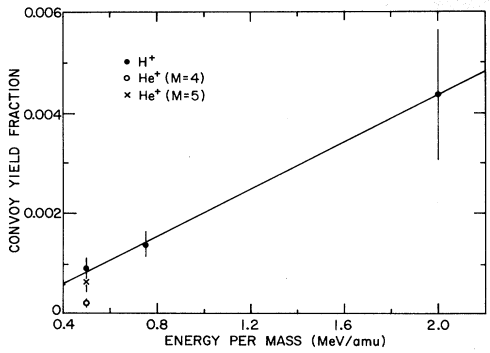

FIG. 12. Ratio of the parameters Y_c/a from Table I as a function of the projectile energy. The solid line is a best-fit straight line to the H^+ data.

simple linear energy dependence of these ratios. As noted, this implies similar velocity dependence of the convoy and high-Rydberg-state production processes. The helium data, however, depart from this picture. It should be noted that by changing the threshold scaling to $1/n^5$, as has recently been suggested for nonhydrogenic atoms,[25,28] the helium data can be brought into line with the hydrogen data. This result is somewhat puzzling because the two-electron fraction of the outgoing helium beam is so small ($<1\%$ of the one-electron fraction).[48] This change ($m=5$) does not significantly affect the conclusion that the capture probability varies as $1/n^3$; however, it decreases the constant a [Eq. (1)] by a factor of 3. The quality of the fit, however, is worse for the case $m=5$ than for $m=4$. For He^+, chi-squared is increased by a factor of 4 for $m=5$.

It is interesting to compare the restricted yield of convoy electrons which we measure to the fitted Rydberg yields. As has been pointed out previously,[33] the mechanism which is responsible for the production of cusp electrons should also be that responsible for the production of the highest-lying Rydberg states below the ionization threshold. As a result, the cross section for capture, per unit energy interval, should be continuous across the ionization threshold. This has already been demonstrated for the case of cusp electrons.[33] These arguments should also apply to the production of convoy electrons in solids. From such an argument, we expect the ratio of our measured yield of convoy electrons to that of Rydberg atoms to be given by the ratio of the range of excitation energies in these measurements. For convenience, we consider the yield of Rydberg atoms with principal quantum numbers >50. These atoms cover a range of ~ 5 meV in binding energy. For 750-keV proton impact, beam-velocity electrons would emerge at 410 eV. Our angular acceptance of $\pm 0.47°$ limits us to observing electrons with <27-meV energy associated with transverse motion in the projectile frame. We therefore would expect to observe five times as many convoy electrons within this acceptance as we do Rydberg atoms with $n>50$. In actual fact, one should expect a slightly higher ratio since the cutoff on the energy associated with longitudinal motion should not have been assumed to be the same as the transverse limit. From the values of a and Y_c given in Table I we find a measured ratio of 7:1, in rough agreement with this estimate.[51]

Another aspect of these data comes from comparing the published one-electron fractions to our extrapolated $n=1$ yields based on the observed Rydberg populations. For our target thickness of 100 Å, the H^0 fractions are not yet equilibrated.[49] Based on the fraction of the one-electron yield which we observe in our extrapolated yield, we would argue that the Rydberg fraction (for the 2-MeV H^+ beam) is produced in the last 17 Å of the target. This can be compared to the escape depth of free electrons in carbon,[52] moving at the beam velocity, which has been found to be 18 ± 6 Å. This observation agrees with the results of Koch[53] who has demonstrated that for high-velocity Rydberg atoms (where the ion velocity is much greater than the Rydberg electron orbital velocity) the Rydberg electron is essentially free, and, therefore, the cross section for collisional destruction of the atom is determined by free-electron scattering.

B. Static fields

The apparatus used for the static longitudinal field measurements was unable to distinguish convoy electrons from those electrons produced by field ionization of high Rydberg-state atoms at the target exit surface. The measurements with this apparatus were therefore carried out in a quench mode. By applying a small electric field to the postdeflectors, beam-velocity electrons created at the target, or in the longitudinal field after the target (see Fig. 1), could be deflected from entering the spectrometer. The electron spectrometer could then be used to detect those Rydberg atoms which survive the longitudinal field but ionize in the stronger spectrometer field. As a function of the longitudinal field strength, these energy spectra form a

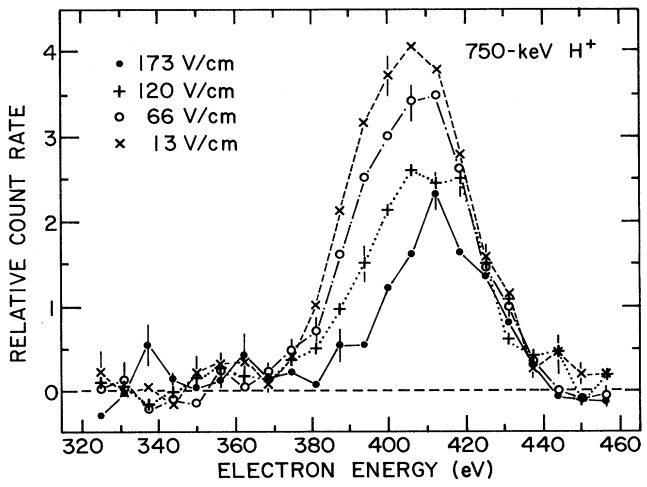

FIG. 13. A comparison of electron energy spectra, measured with longitudinal fields, as indicated, applied immediately after the target as described in text. A weak transverse field (12 V/cm) was used to remove 0° electrons created before the spectrometer entrance. A smooth continuum background has been subtracted to leave the field-ionization signal in the spectrometer.

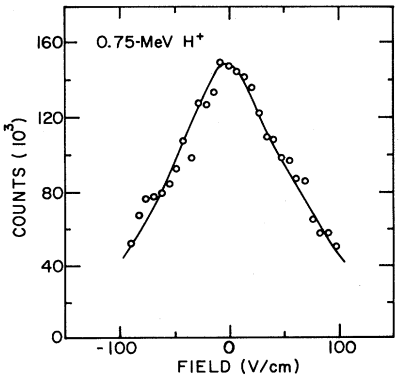

FIG. 14. Yield curve for electrons from the ionization of Rydberg atoms in the spectrometer field as a function of the field applied after the target. The applied field was longitudinal. The Rydberg-state atoms were produced by the impact of 750-keV protons on a 2-$\mu g/cm^2$ carbon foil.

slowly decreasing ridge, similar to the Rydberg ridge of Fig. 3. Figure 13 shows a comparison of these energy spectra for a range of longitudinal field strengths. One observes that the total ionization signal is gradually quenched with increasing longitudinal field. As the longitudinal field increases, the distribution of principal quantum numbers of those surviving atoms is shifted to lower n values. These surviving atoms penetrate further into the spectrometer field before ionizing and thus the centroid of the peak shifts upward in apparent energy. That is, one observes the peak (at increasing longitudinal fields) to be eroded primarily from the low-energy side.

Integration of the residual field-ionization signal observed in the spectrometer, as a function of the longitudinal field strength, gives a measure of the effectiveness of this field arrangement in ionizing the atoms formed by foil excitation. Figure 14 shows a typical curve resulting from such an integration. One sees from the figure a slow falloff of the residual ionization signal with increasing longitudinal field strength. One also observes symmetry of this curve with respect to the direction of the applied longitudinal field.

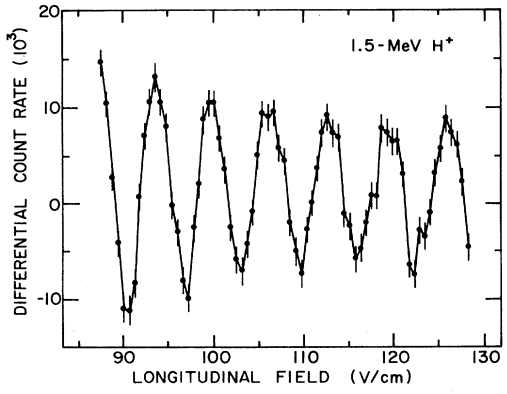

FIG. 15. A differential yield curve obtained with 1.5-MeV proton bombardment. The errors shown are statistical.

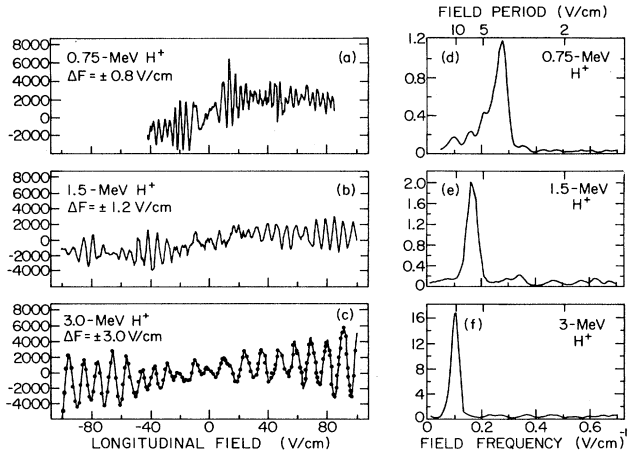

FIG. 16. A comparison of differential yield curves as a function of longitudinal field for three different proton bombarding energies, (a) 0.75, (b) 1.5, and (c) 3 MeV, in the region between ±100 V/cm. The square-wave fields are shown in each. The Fourier power spectrum for each energy is shown in (d), (e), and (f), respectively. The Fourier spectra are computed from the full range of data measured for each energy (not shown).

To investigate this phenomenon more sensitively, we have performed differential measurements.[39] Figure 15 shows typical results of such measurements. The striking oscillations observed do not depend on the frequency of the applied square wave. Moreover, the periodicity with respect to field of these oscillations depends strongly on the velocity of the ion beam as seen in Fig. 16.

The zero level has been determined by removing the square-wave voltage from the target bias. The spectrum was repeated using the same electronic gating conditions. This small correction was applied to the curves presented in Figs. 15 and 16. Since this gives a true zero, one sees from those figures that the ionization signal increases as well as decreases in these quench measurements (the figures actually show the *negative* derivative). Numerical integration of these results produces curves which are in good agreement with the integral quench measurements.[39] From the velocity dependence observed, it is clear that these oscillations do not represent individual ionization thresholds.[15]

We have been able to explain these oscillations within the framework of a simplified model based on first-order perturbation theory for degenerate states.[39] This model assumes that for principal quantum number n, the manifold of n Stark levels is at least partly coherently excited as a result of the interaction with the target. The time-dependent wave function for this coherently excited state will evolve in the longitudinal field immediately after the target as a periodic function of time, with a fundamental frequency proportional to the field strength. For a fixed dwell time in the field, the wave function of the state exiting the field region will be a periodic function of the field strength. When a Rydberg atom enters the tilted field of the spectrometer, this wave function splits into new Stark sublevels. For n near the classical ionization threshold,

the ionization rate in the spectrometer will be a sensitive function of the Stark sublevel population and, hence, of the periodic state exiting the longitudinal field.

We have found excellent agreement of the field periods, for different beam velocities, calculated from this model with those measured.[39] The modulation which we observe in these experiments as a result of this selective excitation of the beam exiting the foil should also be observed in other decay modes of foil-excited ion beams. This might account for previously reported modulations with the electric field seen in the yield of K x rays produced after the passage of the emitting atoms through a longitudinal field.[54,55]

VII. CONCLUSIONS

We have observed the field ionization of highly excited fast-ion beams produced by foil excitation. From the measured yields we find continuity of the capture cross section across the ionization threshold. In measurements with microwave fields, where the applied and stray fields may tend to produce statistical repopulation of the substate population, we find a $1/n^3$ quantum-state population. This is also consistent with measurements of continuum electron cusp shapes[35] which also suggest a $1/n^3$ scaling rule for high-Rydberg-state atoms, near the ionization threshold, formed by electron capture of protons in carbon foils. The states which we observe include coherently excited superpositions of Stark levels. The presence of these states, in fields where the coherency is preserved, could affect measurements of the quantum-state population. This could be the reason that some experimenters have reported somewhat different scaling laws for the measured quantum-state populations of foil-excited beams.[22]

The physical picture which emerges from these observations is that the states we are observing are formed by the capture, into highly excited bound states, by the projectile, of nearly free electrons which move through the foil with the beam, correlated in space and in time. Such a picture leads to the $1/n^3$ population which we observe.

These observations have an important impact on several fields of research. It seems evident from these results that, in interpreting observations on convoy electrons, it is necessary to take into account the possible contributions of electrons stemming from the ionization of projectile Rydberg atoms. It is likely that many of the unresolved puzzles[31] of such research (e.g., simultaneous broad and narrow components,[56] molecular effects,[57] the behavior of the cusp line shape with projectile velocity, etc.) are at least partially due to contributions by field-ionizing Rydberg atoms.

The beam-foil cascade problem is another area where these observations should be important. Cascade calculations of the yield of delayed x-rays from foil-excited ion beams are quite sensitive to the assumed quantum-state populations in the beam, particularly with respect to angular momentum.[6] These phenomena offer a new and potentially powerful technique for studying the excitation mechanisms which produce high Rydberg states of fast projectiles as they exit solids. As such they represent a useful probe of both the ion-solid and ion-surface interactions.

ACKNOWLEDGMENTS

This work was supported by the U.S. Department of Energy, Office of Basic Energy Sciences, under Contract No. W-31-109-Eng-38. Three of us (P.M.K., D.R.M., and W.V.d.W.) also acknowledge partial support of this work by the U.S. National Science Foundation Grant No. PHY80-26548, as well as the hospitality of the entire staff at the Dynamitron Laboratory of the Argonne National Laboratory. One of us (P.M.K.) gratefully acknowledges receipt of an A.P. Sloan Foundation Fellowship.

*Present address: Weizmann Institute of Science, Rehovot 76100, Israel.

†Present address: Research Institute of Fudan University, Shanghai, People's Republic of China.

‡Present address: Physics Department, State University of New York at Stony Brook, Stony Brook, NY 11794.

[1]See, e.g., *Beam-Foil Spectroscopy,* edited by I. A. Sellin and D. J. Pegg (Plenum, New York, 1976).

[2]H. A. Bethe and E. E. Salpeter, *Quantum Mechanics of One- and Two-Electron Atoms* (Academic, New York, 1957).

[3]J. R. Oppenheimer, Phys. Rev. 31, 349 (1928).

[4]R. M. Schechtman, Phys. Rev. A 12, 1717 (1975).

[5]W. J. Braithwaite, D. L. Matthews, and C. F. Moore, Phys. Rev. A 11, 465 (1974).

[6]H.-D. Betz, J. Rothermel, and F. Bell, Nucl. Instrum. Methods 170, 243 (1980).

[7]J. Rothermel, H.-D. Betz, F. Bell, and V. Zacek, Nucl. Instrum. Methods 194, 341 (1982).

[8]H.-D. Betz, J. Rothermel, D. Röschenthaler, F. Bell, R. Schuch, and G. Nolte, Phys. Lett. 91A, 12 (1982).

[9]H.-D. Betz, D. Röschenthaler, and J. Rothermel, Phys. Rev. Lett. 50, 34 (1983).

[10]P. J. Cooney, D. S. Gemmell, W. J. Pietsch, A. J. Ratkowski, Z. Vager, and B. J. Zabransky, Phys. Rev. A 24, 746 (1981).

[11]D. S. Gemmell, Nucl. Instrum. Methods 194, 255 (1982).

[12]P. M. Koch and D. R. Mariani, Phys. Rev. Lett. 46, 1275 (1981).

[13]P. M. Koch, in *Rydberg States of Atoms and Molecules,* edited by R. F. Stebbings and F. B. Dunning (Cambridge University, New York, 1983).

[14]D. Banks and J. G. Leopold, J. Phys. B 11, 2833 (1978).

[15]For reviews of that work, see A. C. Riviere, in *Methods of Experimental Physics 7A,* 208 (1968); R. N. Il'in, in *Atomic Physics,* edited by S. J. Smith and G. K. Walters (Plenum, New York, 1973) Vol. 3; and J. E. Bayfield, G. A. Khayrallah, and P. M. Koch, Phys. Rev. A 9, 209 (1974).

[16]D. Kleppner, M. G. Littman, and M. L. Zimmerman, in Ref. 13. More recent theoretical work on the nonhydrogenic Stark effect that couples a density-of-states formalism for hydrogen with quantum defect theory has been presented by D. A. Harmin, Phys. Rev. A 26, 2656 (1982). Detailed measurements of the ionization of Rydberg triplet states of helium atoms that are partially interpreted using Harmin's theory are being submitted to Phys. Rev. A by W. Van de Water, D. R. Mariani, and P. M. Koch.

[17]T. H. Jeys, G. W. Foltz, K. A. Smith, E. J. Beiting, F. G. Kel-

lert, F. B. Dunning, and R. F. Stebbings, Phys. Rev. Lett. 44, 390 (1980).

[18]H. Rausch von Traubenberg, R. Gebauer, and G. Lewin, Naturwissenschaften 18, 417 (1930).

[19]A. C. Riviere and D. R. Sweetman, *Atomic Collision Processes, Proceedings of the 3rd International Conference on Physics of Electronic and Atomic Collisions,* London, 1963, edited by M. R. C. McDowell (North-Holland, Amsterdam, 1964), p. 734; J. Kingdon, M. F. Payne, and A. C. Riviere, J. Phys. B 3, 552 (1970).

[20]K. H. Berkner, S. N. Kaplan, G. A. Paulikas, and R. V. Pyle, Phys. Rev. 138, A410 (1965).

[21]K. H. Berkner, I. Bornstein, R. V. Pyle, and J. W. Stearns, Phys. Rev. A 6, 278 (1972).

[22]C. J. Latimer, R. G. McMahon, and D. P. Murtagh, Phys. Lett. 87A, 232 (1982).

[23]K. G. Harrison and M. W. Lucas, Phys. Lett. 33A, 142 (1970).

[24]P. M. Koch, J. de Phys. (Paris) Colloq., Suppl. 11, 43, C2-187 (1982).

[25]D. R. Mariani, W. Van de Water, P. M. Koch, and T. Bergeman, Phys. Rev. Lett. 50, 1261 (1983).

[26]D. R. Mariani, Ph.D. thesis, Yale University, 1983 (unpublished).

[27]D. A. Jones, J. G. Leopold, and I. C. Peroival, J. Phys. B 13, 31 (1980), and references therein.

[28]P. Pillet, W. W. Smith, R. Kachru, N. H. Tran, and T. F. Gallagher, Phys. Rev. Lett. 50, 1042 (1983).

[29]G. B. Crooks and M. E. Rudd, Phys. Rev. Lett. 25, 1599 (1970).

[30]J. Macek, Phys. Rev. A 1, 235 (1970).

[31]M. Breinig, S. B. Elston, S. Huldt, L. Liljeby, C. R. Vane, S. D. Berry, G. A. Glass, M. Schauer, I. A. Sellin, G. D. Alton, S. Datz, S. Overbury, R. Laubert, and M. Suter, Phys. Rev. A 25, 3015 (1982).

[32]R. Shakeshaft and L. Spruch, Rev. Mod. Phys. 51, 369 (1979).

[33]M. Rødbro and F. D. Andersen, J. Phys. B 12, 2883 (1979).

[34]V. N. Naelavathi, R. H. Ritchie, and W. Brandt, Phys. Rev. Lett. 33, 302 (1974). W. Brandt and R. H. Ritchie, Phys. Lett. 62A, 374 (1977).

[35]M. W. Lucas, W. Steckelmacher, J. Macek, and J. E. Potter, J. Phys. B 13, 4833 (1980).

[36]Z. Vager, B. J. Zabransky, D. Schneider, E. P. Kanter, Gu Yuan-Zhuang, and D. S. Gemmell, Phys. Rev. Lett. 48, 592 (1982).

[37]B. J. Zabransky, P. J. Cooney, D. S. Gemmell, E. P. Kanter, and Z. Vager, Rev. Sci. Instrum. 54, 531 (1983).

[38]N. Stolterfoht, D. Schneider, and P. Ziem, Phys. Rev. A 10, 81 (1974).

[39]Z. Vager, E. P. Kanter, D. Schneider, and D. S. Gemmell, Phys. Rev. Lett. 50, 954 (1983).

[40]E. P. Kanter, D. Schneider, and Z. Vager, Phys. Rev. A 28, 1193 (1983).

[41]J. E. Bayfield and P. M. Koch, Phys. Rev. Lett. 33, 258 (1974).

[42]P. M. Koch, L. D. Gardner, and J. E. Bayfield, p. 829 in Ref. 1.

[43]J. E. Bayfield, L. D. Gardner, and P. M. Koch, Phys. Rev. Lett. 39, 76 (1977).

[44]P. M. Koch, Phys. Rev. Lett. 41, 99 (1978).

[45]P. M. Koch and D. R. Mariani, J. Phys. B 13, L645 (1980).

[46]J. E. Bayfield, Prog. Quantum Electron. 6, 219 (1980).

[47]A. Chateau-Thierry and A. Gladieux, in *Atomic Collisions in Solids,* (Plenum, N.Y., 1975) Vol. 1, pg. 307.

[48]J. C. Armstrong, J. V. Mullendore, W. R. Harris, and J. B. Marion, Proc. Phys. Soc. (London) 86, 1283 (1965).

[49]M. J. Gaillard, J.-C. Poizat, A. Ratkowski, J. Remillieux, and M. Auzas, Phys. Rev. A 16, 2323 (1977).

[50]R. Laubert, I. A. Sellin, C. R. Vane, M. Suter, S. B. Elston, G. D. Alton, and R. S. Thoe, Nuc. Instrum. and Meth. 170, 557 (1980).

[51]These observations resolve the question of the absolute yields of field-ionizing Rydberg atoms contributing to convoy electron energy spectra. See, e.g., several comments on Ref. 31 in Phys. Rev. Lett. 50, 1014 (1983).

[52]M. P. Seah and W. A. Dench, Surf. and Interface Anal. 1, 2 (1979).

[53]P. M. Koch, Phys. Rev. Lett. 43, 432 (1979).

[54]C. F. Moore, W. J. Braithwaite, and D. L. Matthews, Phys. Lett. 47A, 353 (1974).

[55]P. Richard, C. L. Cocke, S. J. Czuchlewski, K. A. Jamison, R. L. Kauffman, and C. W. Woods, Phys. Lett. 47A, 355 (1974).

[56]A. Gladieux and A. Chateau-Thierry, Phys. Rev. Lett. 47, 786 (1981).

[57]V. H. Ponce, E. González Lepera, W. Mechbach, and I. B. Nemirovsky, Phys. Rev. Lett. 47, 572 (1981).